



Dynamic and spatial behavior of a corrugated interface in the driven lattice gas model

Gustavo P. Saracco*, Ezequiel V. Albano

Instituto de Investigaciones Fisicoquímicas Teóricas y Aplicadas (INIFTA), UNLP, CCT La Plata - CONICET, Casilla de Correo 16 Sucursal 4 (1900) La Plata, Argentina¹

ARTICLE INFO

Article history:

Received 23 December 2009

Received in revised form 4 May 2010

Available online 15 May 2010

Keywords:

Non equilibrium systems

Dynamical interface behavior

ABSTRACT

The spatiotemporal behavior of an initially corrugated interface in the two-dimensional driven lattice gas (DLG) model with attractive nearest-neighbors interactions is investigated via Monte Carlo simulations. By setting the system in the ordered phase, with periodic boundary conditions along the external field axis, i.e. horizontal, and open along the vertical directions respectively, an initial interface was imposed, that consists in a series of sinusoidal profiles with amplitude A_0 and wavelength λ set parallel to the applied driving field axis. We studied the dynamic behavior of its statistical width or roughness $W(t)$, defined as the root mean square of the interface position. We found that $W(t)$ decays exponentially for all λ and lattice longitudinal sizes L_x , i.e., the lattice side that runs along the axis of the external field. We determined its relaxation time τ , and found that depends on λ as a power law $\tau \propto \lambda^p$, where p depends on the temperature and L_x . At low T 's ($T \ll T_c(E)$) and large L_x , p approaches to $p = 3/2$. At intermediate T 's ($T < T_c(E)$), p decreases up to $p \approx 1$, and is free of finite effects. This indicates that the interface stabilizes faster than in the equilibrium model, i.e. the Ising lattice gas ($E = 0$) where $p = 3$. At higher T 's p increases for $T \lesssim T_c(E)$, and the finite size dependence is recovered. Also, if T is fixed, p increases with L_x until it saturates at large values of it, while this regime is vanishing at $T \lesssim T_c(E)$. In this way, the dynamic relaxation process of a sinusoidal interface is improved by the external driving field with respect to its equilibrium counterpart, if the system is set in an intermediate temperature stage far from $T_c(E)$ and in a lattice with a sufficiently large longitudinal side. The behavior of τ was also investigated as a function of E and in the intermediate stage $T < T_c(E)$. It was found that τ decreases exponentially with E in the interval $0 < E \lesssim 1$, while for higher fields it remains constant. The exponential decay depends on the wavelength of the initial profile.

In order to study the spatial evolution of the profiles, we evaluated the structure factor of the interface, and the Fourier coefficients corresponding to the same wave vector of the initial profile. The obtained results allowed us to conclude that the spatial evolution of the profile maintains its initial wavelength, does not travel along the external field axis, and its shape is preserved over all the relaxation process.

© 2010 Elsevier B.V. All rights reserved.

1. Introduction

In the last decades, the study of surface morphology has become a subject of great interest. The theoretical and experimental understanding of the properties of surfaces and interfaces has allowed the development of a large number

* Corresponding author.

E-mail address: gsaracco@inifta.unlp.edu.ar (G.P. Saracco).

¹ <http://www.gfc.inifta.unlp.edu.ar>.

of new technologies that have been applied to generate engineered interfaces in diverse fields such as biology, medicine, metallurgy, catalysis, development of materials, etc. Very recently, the investigation of surfaces at the nanometer scale has added a new and growing collection of interesting and challenging phenomena from both the theoretical and experimental points of view [1–3].

The relaxation process of an initially corrugated surface on its path to equilibrium was early studied by Mullins, who developed a continuum linear theory for the relaxation process of a periodic grooved surface [4]. In this description, the surface evolution of is governed by two competing processes, namely evaporation–condensation (EC) and surface diffusion (SD). If EC is relevant, the surface follows a diffusion equation, where the diffusion constant D depends on the temperature, the vapor pressure above the surface, and also of the mass and volume of the particles. On the other hand, if the surface morphology is changed by SD, the time derivative of the surface height $h(x, t)$ is proportional to the fourth-order spatial derivative of it, the proportionality constant F depends on the surface diffusion constant, the number of particles per surface area, their mass and volume, and also on the temperature and vapor pressure. If the initial condition consists of a one-dimensional sinusoidal profile $h(x, t = 0) = A_0 \sin(kx)$, with a Fourier mode $k = 2\pi/\lambda$ of wavelength λ , the solutions of the equations describing both processes are the following:

$$h(x, t) = A_0 \sin(kx)e^{-Bk^p t}, \quad (1)$$

where $B = D$ or F , and $p = 2$ or 4 if EC or SD, respectively, is relevant. Eq. (1) predicts that the surface amplitude decays exponentially without changing the spatial shape, independently of the Fourier mode under consideration. Also, the relaxation time τ of the surface is proportional to the profile wavelength, i.e., $\tau \propto \lambda^p/B$. These equations are known to hold for temperatures above the roughening transition, $T > T_R$, where all thermodynamic quantities are assumed to be smooth. For the case of surfaces below T_R , the surface free energy and the mobility are singular functions of the reference orientation angles (for example (111) in an fcc solid). By proposing the simplest functional forms for these, the equation that governs the surface evolution, for the EC case, was developed by Selke and Duxbury [5], and the relaxation for an initial sinusoidal profile is the following:

$$h(x, t) \sim (t/\lambda)^{-1/2} \Psi(x/\lambda), \quad (2)$$

that is, the height decays as a power law, and Ψ is a function that exhibits a nonparabolic sharpening at its apexes [5]. Along these years, there has been a large number of studies devoted to confirm Mullins' ideas not only theoretically but also experimentally [6–16].

On the other hand, the general case of interfaces out the small slope limit has also been considered recently. A vectorial stochastic equation was proposed for the evolution of one-dimensional interfaces [17]. It has been shown that an initial sinusoidal profile decays nonexponentially, together with the spontaneous formation of overhangs. These findings were confirmed later by Monte Carlo simulations by considering an Ising-like model in a triangular lattice with conserved density [18]. This result is important because it established the validity of a discrete approach in order to test a theoretical prediction obtained from a continuum equation.

Another subject that has received attention is the relaxation of surfaces that are intrinsically driven out of equilibrium by the application of external driving fluxes (of energy, momentum, mass, etc.) that run parallel to them. This research aims to understand the “healing” of surface defects due to the reduction of the lifetime of instabilities by external agents. Tomar et al. theoretically analyzed the evolution of a conducting crystalline solid where both an electric field and mechanical stress were applied. By using combined techniques of linear stability analysis and self-consistent dynamic simulations, the electromigration caused by the electric field can stabilize the surface morphology against the cracks originated by the mechanical stress that tends to destabilize it [19]. Within this context, much progress has also been achieved by considering simple models that are expected to catch the essential nonequilibrium physics, such as the driven lattice gas (DLG) model introduced by Katz, et al. [20]. The DLG model assumes particles in a square lattice, settled into a thermal bath, and exchanging places with empty neighbors by means of Ising-like attractive interactions due to the absence of long-range order even at low temperatures. These interactions are realized according to Metropolis rules [21], and the boundary conditions are periodic along all directions. Furthermore, an external driving field E is applied in one fixed lattice direction. In this way, the system gives (receives) energy to (from) the thermal bath (applied field). In the long-time regime, the system achieves **nonequilibrium steady states** (NESS) that are characterized by a constant flux of particles directed in the driving field direction. If the temperature of the thermal bath is high enough, the DLG model exhibits lattice-gas-like disordered states. However, at low temperatures an ordered (anisotropic) NESS emerges. This phase is characterized by the presence of strips of high particle density crossing the lattice in the direction parallel to the external field. So, for half-density of particles and at a well-defined critical bulk temperature T_c , the DLG model undergoes a second-order phase transition [22]. Extensive Monte Carlo simulations have shown that T_c increases with the magnitude of E starting from the critical temperature of the Ising model found by Onsager, $T_c^0 = 2.269 \text{ J}/k_b$, which corresponds to $E = 0$, and saturates at $T_c \simeq 1.41T_c^0$ in the limit $E \rightarrow \infty$ [22].

The interfacial behavior of the DLG in the ordered phase has been studied extensively. Some research has shown that the roughening transition is apparently suppressed [23–26], but recent investigations seem to exclude this behavior [27]. Other studies have investigated the behavior of the interfacial modes in an undulated interface when a perpendicular current of particles sets in, recreating the quenching of the system to a very low temperature. By imposing a continuity

equation for the concentration field of each phase, with the current term proportional to both the chemical potential and the external field, but neglecting thermal noise effects, the stability of an initially flat interface perturbed by a traveling wave was analyzed, constraining it to be in local equilibrium [28]. The dispersion relation $\omega(k)$ could be calculated, and it was found that a perpendicular current can destabilize the interface provided that its wavelength is long enough. Also, the external field affects the k -dependence of the real part of ω ($\text{Re}(\omega(k))$), changing the growth or decay rate of the profile (also exponential like in Eq. (1)) with respect to the equilibrium case. The imaginary component of $\omega(k)$ does not vanish if the conductivities of each phase are assumed to be different (called asymmetric model) [28,29]. This introduces a modulation in the rate with the presence of traveling waves. If the perpendicular current is removed, there is no interface instability, and the relaxation rate behaves as $\text{Re}(\omega(k)) \sim -k^{2.5}$ for $E/k \gg 1$, and $\text{Re}(\omega(k)) \sim -k^{3.0}$ for $E/k \ll 1$, i.e., identical to the $E = 0$ case, as estimated theoretically [30–32]. Later on, numerical Monte Carlo simulations on the asymmetric model at very low temperature allowed going beyond the linear regime of the stability analysis [29]. The obtained results supported the existence of traveling waves, and suggested that the external field stabilizes the interfaces by incrementing the surface tension [29]. Subsequently, a new theoretical approach developed to study the stability of a nonequilibrium interface between two coexisting solid phases was considered. This description started from the coarse-grained level through a Cahn–Hilliard equation in the presence of a weak external field, whose orientational dependence on the interface was considered [33]. For small k , $\omega(k)$ is a function of this dependence, plus a term due to the surface currents that sets a length scale of the perturbation decay in the bulk. As special case, in the small slope limit $\omega(k) \propto \pm k^2$ if the field is *normal* to the interface. So, the perturbation becomes unstable (plus sign) if the field is directed from the low concentration phase to high concentration phase, and stable (minus sign) otherwise. This was later confirmed by Szabó et al. by using the DLG model with attractive next and next-nearest interactions [34]. On the other hand, $\omega(k) \propto -k^{3/2}$ if the field is *tangent* to the interface [33]. In another work, Szabó revisited the subject, and proposed a simpler formalism by focusing on the effect of mass transport along the interface. By imposing that the interface motion is determined by particle conservation and assuming that the (particle) current is proportional to the chemical potential along the interface, a perturbed planar interface becomes unstable for all k 's that are less than a characteristic k_0 , which depends on the magnitude of the driving field normal to the interface [35]. As in the case of the results of Yeung et al., the instability disappears with the reversal of the field direction, and the interface also becomes stable if the vertical drift is negligible or suppressed. So, for this case one has $\omega \propto k^4$. However, in spite of the extensive work done, none of these theoretical descriptions have explicitly considered the effects of thermal fluctuations on the interface dynamics.

In view of the studies summarized above, our aim is to describe the dynamic and spatial evolution of initially sinusoidal interfaces with an integer number of wavelengths in the DLG model as a function of the temperature. So, considering them as taking part of a Fourier decomposition of a general profile in a finite sample, we will have an estimation of the time required to wash out the initial structure by converting it into an essentially flat surface, i.e., with the characteristic roughness at the considered T . Also, the discrete nature of our model and possible nonlinearities in the interfacial behavior were not considered by the analyses above summarized [28,33,35]. Some possible ways to overcome this should be to propose a phenomenological-based equation of the interface height, as for example the KPZ equation [36] including temperature fluctuations, or to investigate the evolution of interfaces in analogous versions of the DLG model developed by Díez-Minguito et al. [37] or Siders [38], that considered off- and on- driven lattice models with different particle interactions, for example a Lennard–Jones or square-well attractive potentials, and compare the obtained results with our model's and the analytic ones. However, these models have, in general, a behavior that is not similar to the discrete version, for example the decrease of the critical temperature with the field strength [37], or the disappearance of the stripe configuration when the lattice potential is zero [38], that reduces the model to a driven fluid with square-well interactions. In another but similar context, research of this kind has been done by Castez et al. where the most relevant results from the linear theory of surface diffusion are recovered by Monte Carlo simulations [17,39].

The paper is organized as follows: in Section 2 the DLG model and the starting configuration are described; the simulation of the model and the measured observables are explained in Section 3; our results are presented and discussed in Section 4, and finally the conclusions are stated in Section 5.

2. The model

The DLG model [20] is defined in a square lattice of size $L_x \times L_y$. The driving field (E) is applied along the x -direction. In this case, the boundary conditions are periodic along the field axis, and closed along the y -direction. This means that the particles at the $y = 1$ edge can not jump into an empty site at $y = L_y$ edge, and vice versa. This modification of the original boundary condition was performed to keep the bottom edge (i.e the flat interface, see left panel of Fig. 1) occupied with particles, a condition that is needed for the interface identification algorithm. Each lattice site can be empty or occupied by a particle. If the coordinates of a site are (i, j) , then the label (or occupation number) for that site can be $\eta_{ij} = \{0, 1\}$. The set of all occupation numbers specifies a particular configuration of the lattice. The particles interact among them through a nearest-neighbor attraction with positive coupling constant $J > 0$. So, in the absence of any field, the Hamiltonian is given by

$$H = -4J \sum_{\langle ij:i'j' \rangle} \eta_{ij} \eta_{i'j'}, \quad (3)$$

where $\langle . \rangle$ means that the summation is made over nearest-neighbor sites only.

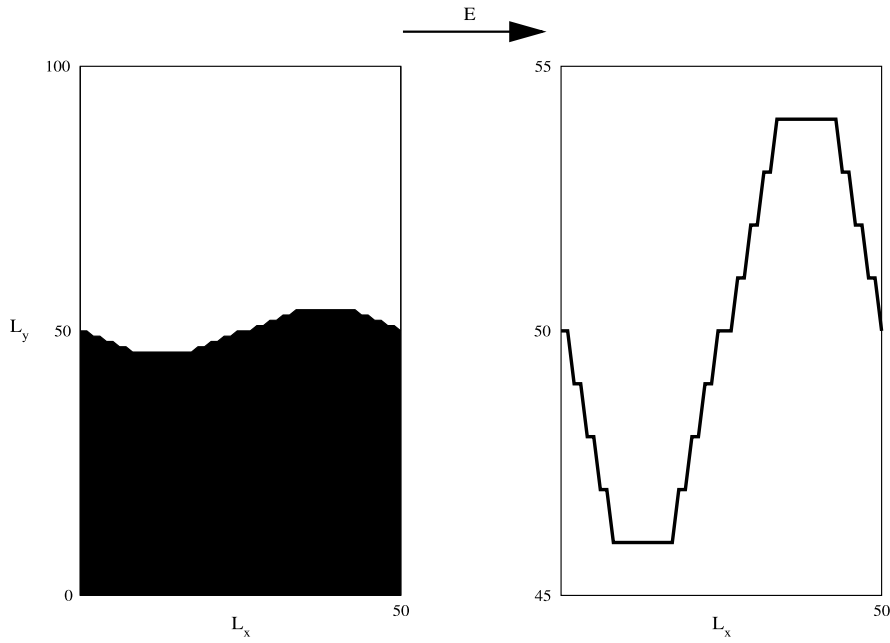


Fig. 1. Left panel: initial configuration of the DLG model in a lattice of sides $L_x = 50$, $L_y = 100$, with $\lambda = 50$ and $A_0 = 5$. The black region is the particle stripe with $\rho = 1/2$. Right panel: Amplified plot of the initial sinusoidal profile in the configuration of the left panel. The external field direction is indicated by the arrow.

The attempt of a particle to jump to an empty nearest-neighbor site (P_{jump}) is given by the Metropolis rate [21] modified by the presence of the driving field, that is,

$$P_{jump} = \min[1, e^{-[\Delta H - \epsilon_1 E]/k_B T}], \quad (4)$$

where k_B is the Boltzmann constant, T is the temperature of the thermal bath, ΔH is the energy change after the particle–hole exchange, $\epsilon_1 = (-1, 0, 1)$ is a number that indicates the direction of jump of the particle against, orthogonal or along the driving field E . The field is measured in units of J , and temperatures are given in units of J/k_B . The dynamics imposed does not allow elimination of particles, so the density is a conserved quantity (i.e., Kawasaki dynamics). Also, it is important to mention that due to particle–hole symmetry, the behavior of holes in the condensed phase is identical to particle behavior in the condensed phase.

In order to investigate the evolution of a corrugated interface, the initial condition of the system that exhibited in the left panel of Fig. 1 (the black region represents the particle stripe). Also, an amplified plot of the sinusoidal profile is shown in the right panel, which has the following expression:

$$h(x, 0) = \frac{L_y}{2} - A_0 \sin\left(\frac{2\pi}{\lambda}x\right), \quad (5)$$

where A_0 is the amplitude and λ is the wavelength of the profile. In all cases the density of particles is kept constant at $\rho = 1/2$.

In the DLG model, the properties and even the existence of interfaces depend on the temperature T . In fact, for $T \geq T_c(E)$, the system is in the disordered phase and there are no interfaces at all. However, for $T < T_c(E)$, interfaces are present due to the strip-like patterns characteristic of the ordered phase. The particles at the interfaces may leave the strip, diffusing into the gas-like phase, or may stick to it again. Moreover, the driving field sets a current along the interface. These processes may change the interface width W (see Eq. (6)). It is well known that W is the result of two contributions, namely the intrinsic width of the interface, W_{in} , of the order of the bulk correlation length ξ_B , and the thermal fluctuations of the local mean position of the interface, i.e., the capillary waves [24]. If the system is in the rough phase and far from the critical point, $T_R < T \ll T_c(E)$, W_{in} is negligible, and the interface evolution is governed by the fluctuations of the capillary waves. On the other hand, if $T_R \ll T \lesssim T_c(E)$, the bulk correlation length becomes relevant, W_{in} is no longer negligible, and mounts over the capillary waves, making W to increase in this regime, causing the relaxation time τ of the sinusoidal profile to be larger than in the $T_R < T \ll T_c(E)$ interval.

3. The simulation method

The model was simulated in square lattices of sizes $L_x \times L_y$, with $L_y = 100$ lattice units (LU) fixed, and L_x in the range $50 \leq L_x \leq 10^4$ (LU). The system was allowed to evolve over very long time intervals, typically $t \geq 1 \times 10^6$ Monte Carlo steps (MCS), defined as $L_x \times L_y$ attempts for a randomly chosen particle to jump into a neighboring site.

We investigated the interface behavior of the model in the temperature range $0.5 \leq T \leq 2.5$, in units of J/k_B . The external field was measured in units of the coupling J , and varied in the range $0.1 \leq E \leq 10$. The profile amplitude A_0 was fixed at $A_0 = 5$ for all simulations, and the wavelength was varied according to $\lambda = L_x/n_\lambda$, where n_λ is the (integer) number of sinusoidal profiles included in L_x .

In order to investigate the time evolution of the sinusoidal profile in the DLG model, we measured the *interface width* or *roughness* W . In order to define it, we first need to find the interface position at time $th(i, t)$, with $1 \leq i \leq L_x$ and $1 \leq h(i, t) \leq L_y$. This was determined by using the algorithm developed in Ref. [40] for diffusion fronts, and recently applied to the DLG model [27]. Let us now explain conceptually how it works, by applying a three-stage process. In the first stage, the lattice is swept sequentially from bottom to top (see left panel of Fig. 1), and the largest cluster of particles is identified by applying the standard Hoshen–Kopelman algorithm (HK) [41]. In the second stage, the HK algorithm is repeated but *from top to bottom*, in order to identify the largest cluster of empty sites. At this point, the lattice has only two large clusters, one made of particles only, and a second one made of empty sites. In this way, the interface is defined as those particles of the largest cluster of occupied sites having at least a neighbor site that belongs to the largest cluster of empty sites. One important feature of this method is that it takes into account the bubbles and overhangs responsible for the intrinsic width of the interface. For more details of the algorithm see Refs. [27,40] and references therein.

Once $h(i, t)$ was estimated, we compute the *average interface position at time t* and the width $W(t)$, defined as the root mean square of the interface position, i.e.,

$$\langle h(t) \rangle = \frac{1}{N_I} \sum_{i=1}^{N_I} h(i, t), \quad W(t) = \sqrt{\langle h(t)^2 \rangle - \langle h(t) \rangle^2} \quad (6)$$

where N_I is the total number of particles at the interface. Notice that the summation in both quantities runs over all the particles of the interface because in general $N_I \geq L_x$ and hence $h(i, t)$ is not a single-valued function of the x -coordinate due to the presence of overhangs.

To study the spatial evolution of the initially sinusoidal profile, we also measured the *structure factor*, defined as

$$S(k, t) = \left\langle \left| \sum_{i=1}^{L_x} \bar{h}(x, t) e^{i(k \cdot x)} \right|^2 \right\rangle, \quad (7)$$

where $\bar{h}(x, t)$ is converted into a single-valued function by averaging the overhangs of the interface in the column denoted by x in the horizontal field axis.

Finally, in order to obtain more information about the spatial shape evolution of the profile, we also measured and analyzed the Fourier coefficients given by Refs. [8,9]:

$$a_k(t) = \sum_{x=1}^{L_x} \bar{h}(x, t) \sin(kx), \quad b_k(t) = \sum_{x=1}^{L_x} \bar{h}(x, t) \cos(kx), \quad (8)$$

where k is a generic Fourier mode. In this way, one coefficient would be more relevant than the other depending on whether the profile interferes either constructively or destructively with the sine or the cosine functions. Furthermore, both coefficients will carry out the time exponential decay discussed above for the interface width $W(t)$, so the time dependence will be linear.

4. Results and discussion

4.1. Dynamic relaxation

Although the interface identification algorithm has proved to be reliable for the DLG model [27,40], we will begin this section by checking the evolution of the interfaces for the case at $E = 0$, which is the widely-studied Ising-like equilibrium lattice gas (EqLG) model, which corresponds to model B in the classification of Hohenberg and Halperin [42]. In the left panel of Fig. 2, we observe that the amplitude actually decays with time, and the sinusoidal shape is roughly conserved. In contrast, when a small field is applied, as shown in the right panel of Fig. 2 with $E = 0.1$, the decay is much faster than that observed for the EqLG model.

The dynamic evolution of the sinusoidal profile can be quantified by measuring the interface width defined by Eq. (6). Fig. 3 exhibits the dynamic evolution of the roughness W of an initially prepared sinusoidal profiles of different wavelengths λ (for the sake of clarity, we do not show the evolution of all profiles considered), in a square lattice of sides $L_y = L_x = 100$, and $T = 1$. It is observed that for $\lambda < 100$, all profile widths reach a minimum value, and then grow up to an equilibrium value $W_\infty = W(t \rightarrow \infty)$ that is independent of the initial state (it only depends on T). For fixed amplitudes as in the case of Fig. 3, the absolute value of the local slopes along the interface becomes larger when λ decreases, and consequently the interface particles are weakly bounded as compared with profiles of longer wavelengths. So, the particles can be driven outside the interface (e.g. to the gas phase) by thermal fluctuations, causing a fast decay. This behavior occurs no matter how large L_x is, so that it is almost independent of the finite size of the sample. At the minimum value reached by $W(t)$ one has a nearly flat interface that is not an equilibrium state of the system compatible with the temperature of the thermal bath.

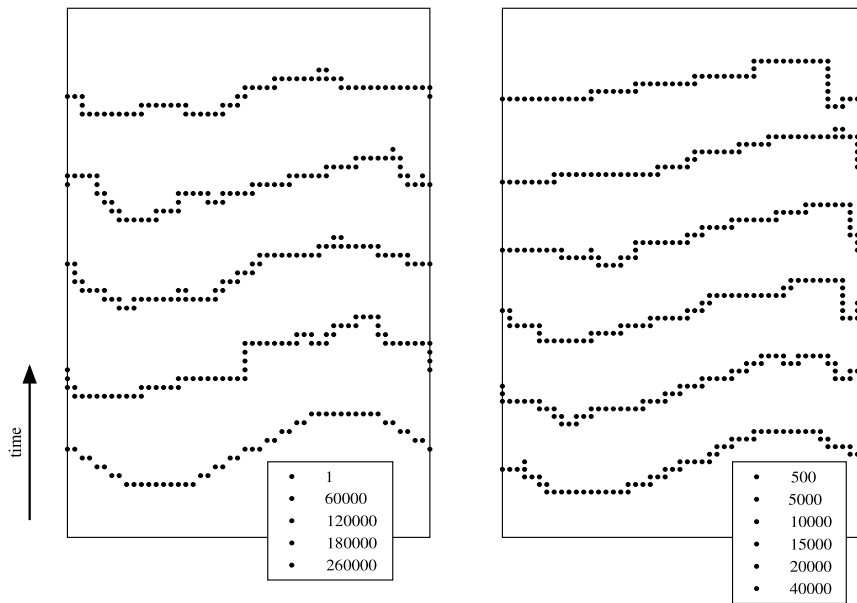


Fig. 2. Interface snapshots, represented by full dots, of the EqLG and DLG models obtained from a starting interface profile of wavelength $\lambda = 50$, in a lattice of sides $L_x = 50$, $L_y = 100$, and $T = 1$, and obtained at the times indicated in the legends. The left panel shows the interface evolution of the EqLG model ($E = 0$), while the right panel shows the time evolution of the interface of the DLG model where a driving field of magnitude $E = 0.1$ is applied from left to right.

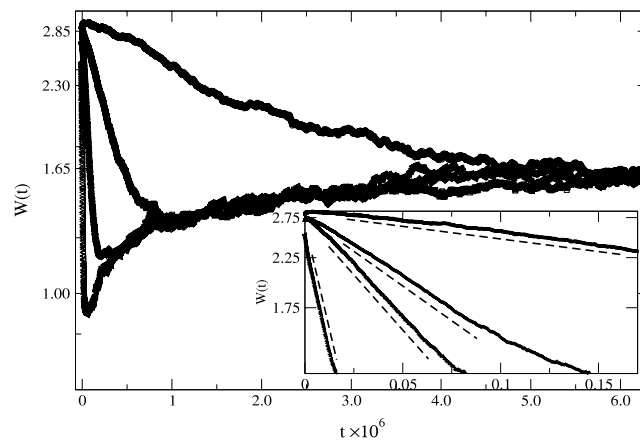


Fig. 3. Dynamic evolution of the interface roughness W as measured for the EqLG model set on a square lattice of sides $L_x = L_y = 100$ LU and $T = 1$. The starting sinusoidal profiles have amplitude $A_0 = 5$ and wavelengths $\lambda = 100, 50, 25$, and 10 , from top to bottom. The data were obtained by averaging over 100 independent samples. The inset shows the exponential fits of the numerical data corresponding to $\lambda = 50, 25, 20$ and 10 (the other fits are not shown to make the plot clearer).

So, $W(t)$ grows again due to thermal fluctuations of the capillary waves, until the equilibrium state is reached in the limit of $t \rightarrow \infty$, i.e., when $W = W_\infty$. We fitted the data with an exponential decay according to $W(t) - W_\infty = B \exp(-Kt)$, where $K = 1/\tau$. The fits of the numerical data, which allow us to estimate the relaxation time τ , are also shown in Fig. 3.

By evaluating τ for the interfaces of systems in lattices of sides $L_x = 100$, $L_x = 500$ and $L_x = 1000$ ($L_y = 100$ in all cases), one can study the behavior of τ with both k and L_x . Fig. 4 shows log–log plots of τ versus the wavelength λ as obtained for the EqLG model. Regression fits of the data are performed in the large λ interval, giving good agreements between the numerical results and the predicted behavior for the exponent $p = 3$ in theoretical descriptions, i.e. $p = 3.03(2)$ for $L_x = 500$ and $p = 3.01(2)$ for $L_x = 1000$ [30–32]. This is confirmed by inset of Fig. 4, that shows a plot of the ratio $\tau^{1/3}/\lambda$ versus λ . Since the wave amplitude was fixed at $A_0 = 5$ for all cases, the obtained behavior indicates us that the predicted power-law behavior is valid within the small slope limit. These results provide a stringent test for the methodology used in order to locate the interface and follow its dynamic evolution.

After the validation of the method, we turn now to the DLG model. Since it is driven out of equilibrium by an external field, one expects that the field may influence the relaxation of the starting sinusoidal profile. This becomes evident in the

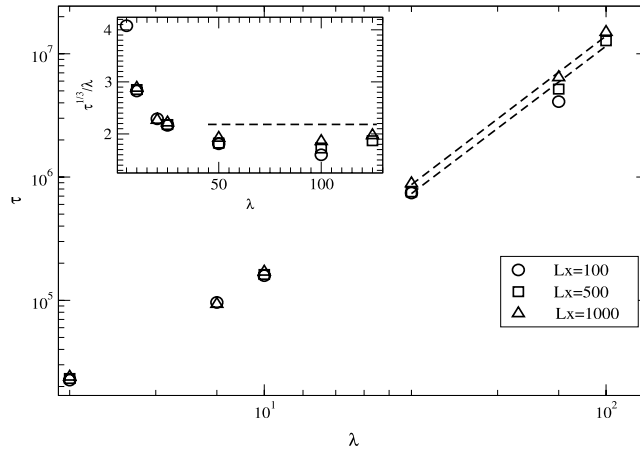


Fig. 4. Log–log plot of the relaxation time τ calculated from the decays of $W(t)$ shown in Fig. 3 for the EqLG model, versus the wavelength λ , as obtained for samples with sides indicated in the legend. The fits with a cubic function are also exhibited for the cases $L_x = 500$ and $L_x = 1000$. Inset: linear–linear plot of the ratio $\tau^{1/3}/\lambda$ versus λ , which indicates the validity of the power-law predicted theoretically [30–32] within the small slope limit ($A_0 = 5$ in all cases). The straight line was plotted to guide the eye.

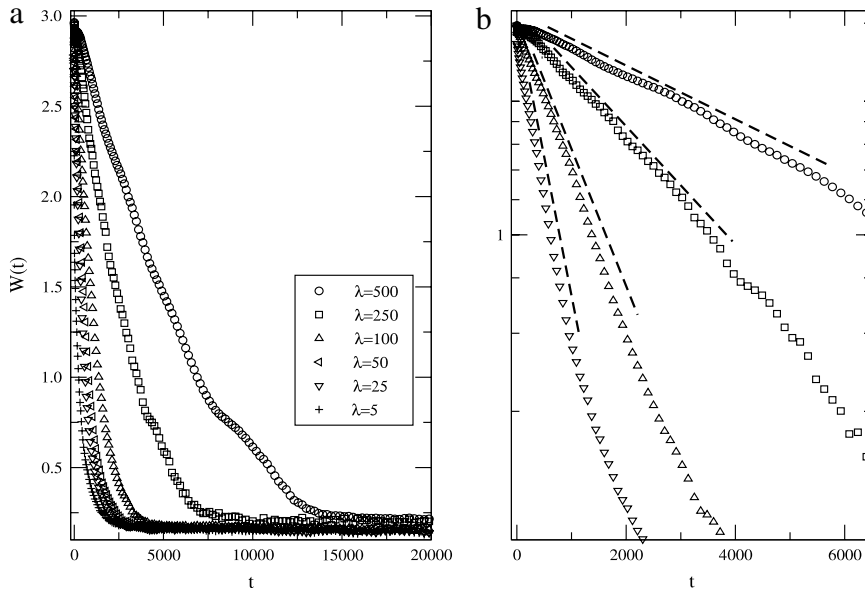


Fig. 5. (a) Dynamic evolution of the interface roughness $W(t)$ (linear–linear scale) for the DLG model with $E = 1$, $T = 1$ as measured by using a lattice of sides $L_x = 500$ and $L_y = 100$. Data obtained by starting from sinusoidal profiles with different wavelengths λ , as indicated in the legend; (b) Log–linear plot of some decays exhibited in (a), together with its corresponding displaced fits with an exponential function (see text).

snapshots of Fig. 2, which shows that the amplitude decay is faster as compared to the case of the EqLG model. Based on the theoretical results of the continuum approaches in Refs. [28,33,35] the dynamic interface roughness amplitude $W(t)$ of the DLG model is expected to decay exponentially for $T > T_R$, $W(t) - W_\infty = B \exp(-t/\tau)$, where τ is the relaxation time, and $W_\infty = W(t \rightarrow \infty)$. Fig. 5(a) and (b) shows the exponential relaxation W , in a lattice with $L_x = 500$, $E = 1$, and $T = 1$, as measured for a series of profiles with different λ 's. Comparing Figs. 5(a) and 3 of the EqLG model, we observe that $W(t)$ decays faster and the minima disappear when more initial sinusoidal profiles are allocated in the lattice, i.e., when λ is shorter.

By fitting the decaying behavior with an exponential function, shown in Fig. 5(b), we measured τ for all wavelengths, even if $A_0/\lambda = 1$. We repeated this for the decay in several lattices of longitudinal sizes $L_x = 100, 200, 500$ and $10,000$ LU, and T 's in the range $0.5 \leq T \leq 2.5$, in order to study the dependence on λ and T .

Fig. 6 shows log–log plots of the estimated values of the relaxation times τ versus the profile wavelength λ , for all the investigated temperatures. The behavior of τ with λ is consistent with a power-law function $\tau \propto \lambda^p$.

The plots in Fig. 7(a) and (b) shows the behavior of p as a function of the temperature T and the longitudinal side L_x , respectively. Fig. 7(a) shows that, in the low temperature regime, $T \leq 0.5$, p increases with L_x , suggesting that p approaches $p = 3/2$ in the limits of large L_x and zero thermal fluctuations, as was theoretically found by Yeung et al. [33]. In the

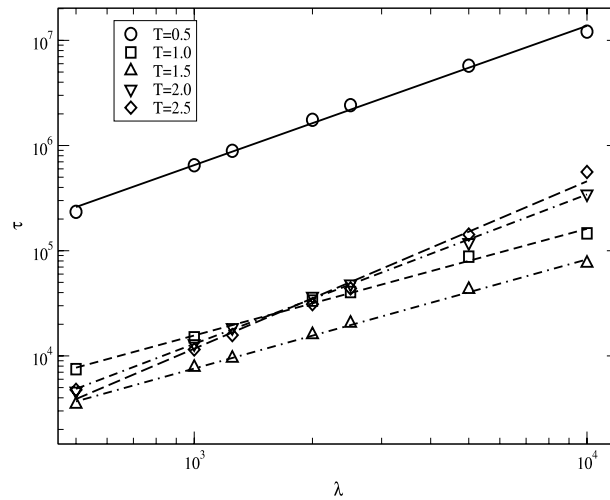


Fig. 6. Log–log plot of the relaxation time τ versus λ for the DLG model with $E = 1$, $L_x = 10,000$, $L_y = 100$, and $A_0 = 5$. Data obtained at different temperatures as indicated in the legend. The straight lines show the power-law fits corresponding to each T investigated.

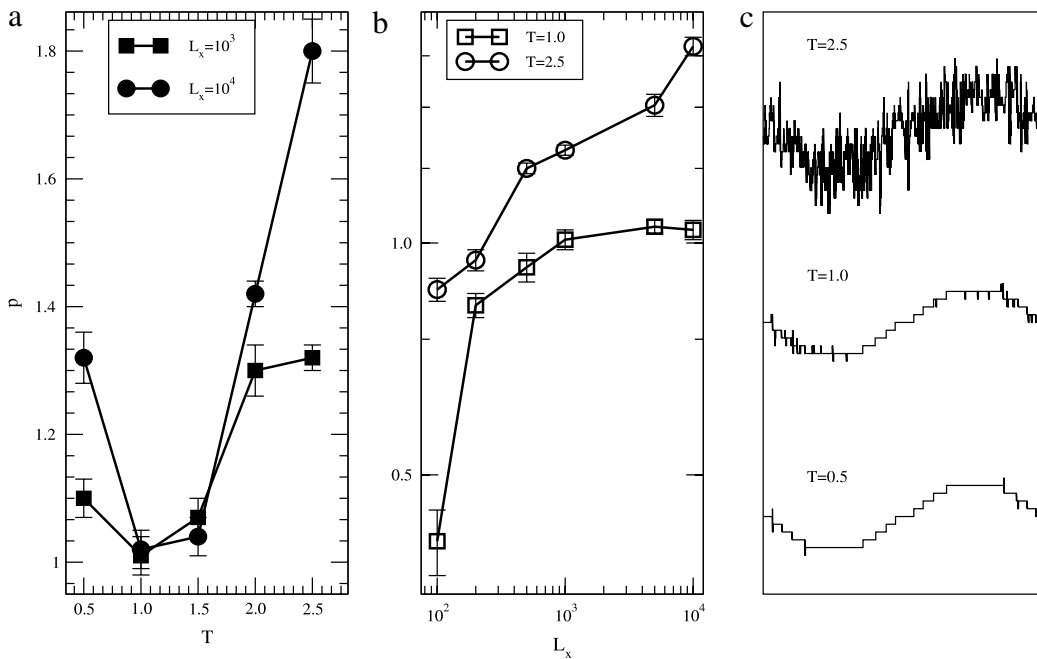


Fig. 7. Dependence of p versus T (a) (in linear–linear scale) and L_x (b) (in log–log scale for clarity). In both cases, we used $E = 1$. The longitudinal lattice sides used in (a), and the temperatures in (b) are indicated in the corresponding legends. The plots in (c) exhibit the interface snapshots taken during the exponential relaxation process at $t = 2500$ MCS, in a system with $L_x = 10^4$, $L_y = 10^3$, and $E = 1$. The temperature of the thermal bath in each snapshot are indicated in the corresponding legends.

intermediate temperature regime $1.0 \leq T \leq 1.5$, the exponent is $p \simeq 1.0$, and it is approximately independent of L_x . In contrast to the former case, the thermal fluctuations become important within this regime, causing the profile to relax faster than in the equilibrium case, i.e., the EqLG model with $p = 3$ (see first part of Section 4.1), and also than the driven model at lower T 's. For higher T 's in the range $1.5 < T \leq 2.5$, p increases due to the fact that T becomes near to the critical temperature $T_c(E = 1) \sim 3.0$ [43], and for $T \gtrsim 1.8$ the finite size effects begin to be noticeable. The increment of p in this regime can be explained by arguing that near T_c , $W(t)$ increases due to the strong contribution of the intrinsic width W_{in} , that is of the order of the bulk correlation length ξ_B [24,27,35]. Consequently, the profile relaxes more slowly to its NESS values than in regimes at smaller T , and it is strongly affected by the finite longitudinal lattice size.

On the other hand, Fig. 7(b) shows the dependence of p with L_x for two temperatures $T = 1, 2.5$, and $E = 1$. For $T = 1$, p increases with L_x until it becomes large, i.e. for $L_x \gtrsim 1000$, where it remains constant (within error bands) around $p \approx 1$. If the

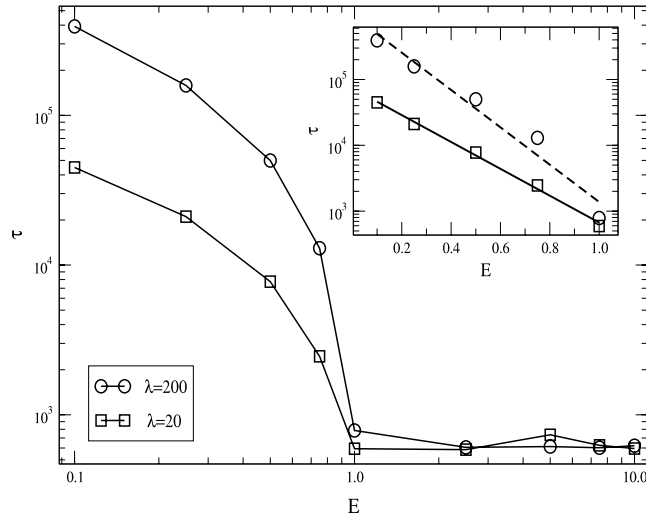


Fig. 8. Relaxation time τ versus the magnitude of the external field E shown on a double logarithmic scale. Data corresponding to the DLG model with $L_x = 200$ and $T = 1$. The amplitude of the initial profiles is $A_0 = 5$, and the wavelengths are indicated in the legend. The inset shows log-linear plots of the data already shown in the main plot, taken within the small field interval. The curves corresponding to different wavelengths are fitted with an exponential function as indicated by full and dashed lines.

temperature of the thermal bath is raised to $T = 2.5$, p grows with increasing L_x , again due to the large values of $W_{in} \sim \xi_B$ already commented. Finally, the behaviors explained above are confirmed by direct observation of the interface snapshots at different temperatures, as 7(c) shows. The increase of $W(t)$ with T , particularly W_{in} , is evident.

By applying external fields of different magnitudes E at fixed $T = 1$, the curve of the relaxation time τ versus E could be obtained for profiles with wavelengths $\lambda = 20$ and $\lambda = 200$ (Fig. 8). It was found that, for small values of E , τ decreases as expected. This process is improved when the profile wavelength is shorter due to the high value of the local slope, where the particles are more weakly attached to the interface than those with longer wavelength. Also, τ follows an exponential decay in the small E regime that depends on λ . To the best of our knowledge, this result appears to be a new feature of nonequilibrium interfaces.

Then, for large values of the field $E \geq 1$, τ reaches a saturation value that is independent of λ . This behavior is due to the fact that movements against the field direction are almost forbidden, and almost all particles at the interface are released into the gas phase, contrary to the case $E < 1$, where the energy that the field needs to extract a particle from the interface competes with the attractive energy between neighboring particles, as denoted in the Hamiltonian of Eq. (3). Also, the crossover point between the decreasing and saturation regimes depends on T , and will occur at larger values of E . This happens because the thermal noise is incremented with higher T 's, (see for example the snapshots in Fig. 7(c)) and a larger value of E will be needed to take a particle away from the interface, avoiding possible re-attachments.

4.2. Spatial behavior

In order to understand the spatial behavior of the profile, it is interesting to study its shape. For this purpose we measured the structure factor of the profile, given by Eq. (7). Fig. 9 shows plots of the structure factor versus the wavelength ($\lambda = 2\pi/k$), for the DLG model in a lattice with $L_x = 500$, $L_y = 100$, $T = 1$, and $E = 1$, as obtained for two profiles with wavelengths $\lambda = 50$ and $\lambda = 250$. As it can be observed from the plots, the structure factors peak at $\lambda = 50$ and $\lambda = 250$, which indicates that each profile decays essentially keeping the same initial wavelength, i.e., maintaining its shape within the short-time regime (see also Fig. 2). Also, the peak of the profile decays faster for the shorter λ 's, confirming our results on the dynamic decay discussed above.

More information on the spatial behavior can be obtained by analyzing the Fourier coefficients $a_k(t)$ and $b_k(t)$, defined by Eqs. (8). Notice that the previous result also impose some constraints on the coefficients a_k and b_k . In fact, on the one hand the evolution of the structure factor allows us to fix the wavevector k of both the sine and cosine functions as equal to that corresponding to the initial profile. On the other hand, Fig. 2 shows that there are not relevant phase shifts during the relaxation process. Fig. 10(a) shows plots of both a_k and the slope $a_k/W(t)$ versus $W(t)$ (since $W(t)$ is a decaying function of time, the horizontal axis must be read from right to left in order to follow the time evolution). A linear dependence can clearly be observed for all wavelengths at early times, although it is different for the profiles with shorter wavelengths ($\lambda = 10, 50$), where the decay is faster than in the other cases. This regime is confirmed by the nearly constant slope $a_k/W(t)$ observed up to $W(t) \cong 1.5$ for long λ 's when $A_0/\lambda \ll 1$. However, the slopes for shorter λ 's reveal that the constructive interference is maintained only at early times due to a faster relaxation.

On the other hand, Fig. 10(b) shows the behavior of the Fourier coefficient $b_k(t)$ and the corresponding slope $b_k(t)/W(t)$ as a function of $W(t)$. At the beginning of the relaxation, b_k is negligible because of the initial pure sinusoidal profiles. Then it

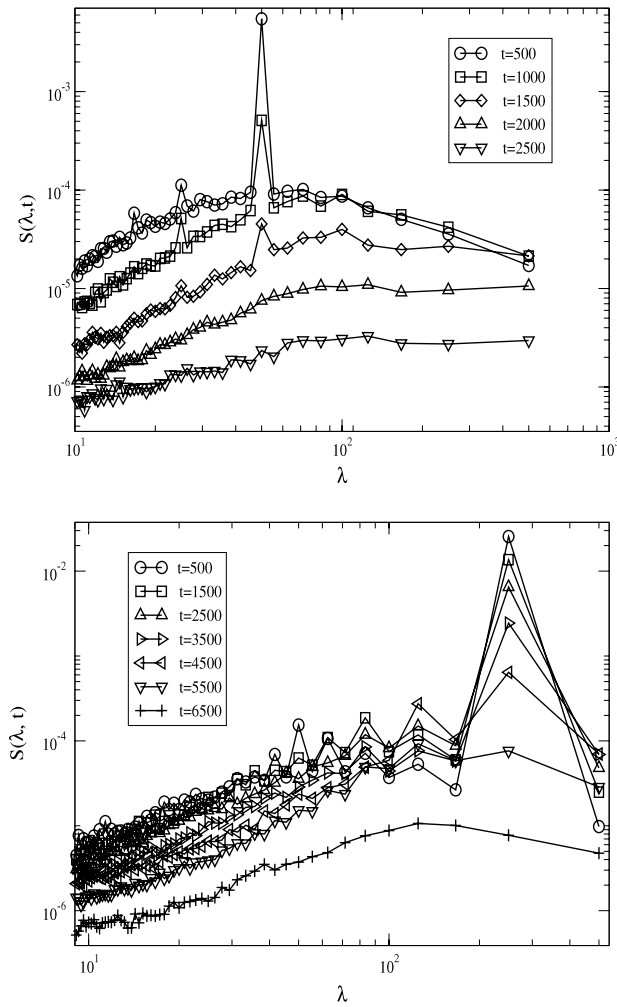


Fig. 9. Log–log plots of the structure factors versus λ for profiles with $\lambda = 50$ (upper panel) and $\lambda = 250$ (lower panel), taken at the times indicated in each legend. The longitudinal side is $L_x = 500$, and the control parameters are $T = 1$ and $E = 1$. The results were obtained by averaging over 500 independent samples.

grows and reaches a saturation value that is practically the same for all λ 's used, until $W(t) \simeq 1$ where it begins to decrease. The corresponding slopes $b_k/W(t)$, shown in the inset, start from zero and grow up to $b_k/W(t) \cong 30$ when $W(t) \simeq 1$ where subsequently they decrease. These results indicate a weak interference of the profile with the cosine function during the relaxation process, which reaches its maximum at $W(t) \simeq 1$. At this value the profiles are close to their saturation values, and no undulatory behavior can be detected either via a_k or b_k , so they both approach zero.

Based on the results exhibited in Fig. 10 we conclude that the predominant constructive interference is observed for the coefficient a_k , since the slope $a_k/W(t)$ is one order of magnitude larger than the values obtained for the corresponding slopes of b_k . In this way, the initial profile has a strong sinusoidal component during all the relaxation process. In other words, the relaxation process also keeps the spatial initial shape, in spite of the external driving field E .

5. Conclusions

In this work a detailed analysis of the evolution of initially corrugated profiles in the two-dimensional driven lattice gas (DLG) model has been performed. By employing Monte Carlo simulations, the evolution of a one-dimensional sinusoidal interface with fixed amplitude $A_0 = 5$ and several wavelengths λ was monitored. The dynamic evolution was studied by measuring the statistical interface width or roughness $W(t)$, in lattices with fixed L_y and several longitudinal sizes L_x for a wide range of temperatures. According to former theoretical works [28,33,35] the time evolution of $W(t)$ in Fig. 5(b) suggests that the interface relaxes exponentially for all the investigated values of T , even for large ratio A_0/λ , so the relaxation time τ can be estimated. It was found also that τ increases with λ as a power law, $\tau \propto \lambda^p$ (Fig. 6), with p depending on the temperature and on L_x , as it is shown in Fig. 7(a) and (b) respectively. In the low temperature regime, p approaches to $p = 3/2$ at larger longitudinal L_x , in good agreement with that theoretically estimated by Yeung et al. [33]. The relaxation

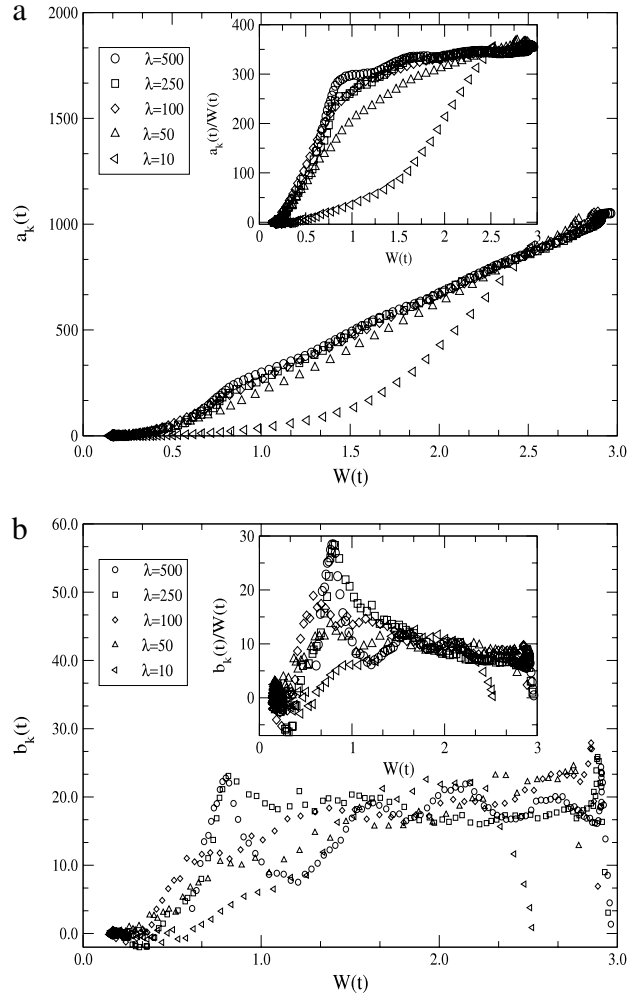


Fig. 10. Linear-linear plots of the Fourier coefficients $a_k(t)$ (a) and $b_k(t)$ (b) and the respective slopes $a_k(t)/W(t)$ and $b_k(t)/W(t)$ (insets of each plot) versus the interface width $W(t)$ as measured for the DLG model in lattices of sides $L_x = 500$, $L_y = 100$, and for $T = 1$ and $E = 1$. The initial amplitude of the sinusoidal profiles is $A_0 = 5$, and their wavelengths λ are indicated in the legends. In order to follow the time evolution of the profile, the horizontal axis must be read from right to left.

process is mainly due to the action of the external field, that enhances it by filling the valleys and smoothing the bumps of the sinusoidal interface. For intermediate temperatures $0.5 < T \leq 1.5p$ decreases up to $p \simeq 1$, and it is practically independent of L_x . The intrinsic width contribution, provided by temperature fluctuations, is small and add to the action of the external field, so the profile relaxes quicker than in the equilibrium and the former cases, respectively. Near the transition temperature of the DLG model ($T = 2 - 2.5$ since the considered driving field magnitude is $E = 1$), thermal fluctuations are strong, the intrinsic width increases, the roughness $W(t)$ becomes larger [27,35], and prevail over the external field effects. Consequently, the relaxation time also becomes larger than in the other cases (at lower T 's), and p increases. Furthermore, its value is affected by the finite size of L_x . On the other hand, Fig. 7(b) shows, for $T = 1$, that p increases with small L_x , but stabilizes for reasonable large values of it, while if $T = 2.5$, p increases with L_x because of the strong contribution of the intrinsic width to $W(t)$ near T_c , causing the profile to decrease slower than at smaller T 's. All these behaviors are confirmed by the interface snapshots at different T 's in Fig. 7(c). Based on these results, we can state that the external field accelerates the relaxation process of a sinusoidal profile if the temperature of the thermal bath is neither near zero nor the critical temperature of the system, and it is free of finite size effects, provided that L_x is large enough, above 1000 LU. Furthermore, the power law behavior $\tau \propto \lambda^p$ gives information on which Fourier modes decay faster in a nonequilibrium interface, which may be useful for the study of more general interfaces far from equilibrium.

Finally, the spatial evolution of the interface was studied. The structure factor, given by Eq. (7), was measured first. The obtained results, shown in Fig. 9, evidence that the wavelength of the profile is maintained over all the relaxation process. Furthermore, the snapshots in Fig. 2 reveal that relevant displacements of the profile along the field axis can clearly be ruled out at this temperature ($T = 1$). This result, together with the conservation of the profile wavelength, became important in the measurement of the Fourier coefficients a_k and b_k defined by the set of Eqs. (8), since no significant phase shifts need to

be added to avoid undesirable destructive interference between the profile and the functions. According to Figs. 2 and 10(a) and (b), it can be concluded that the interface remains static all over the time evolution, and its spatial shape interferes more constructively with the sine function ($a_k(t)$ coefficient) than with the cosine function ($b_k(t)$ coefficient), so the initial profile decays with time by keeping essentially the initial sinusoidal shape.

Acknowledgements

This work was carried out under the support of CONICET, UNLP, and ANPCyT (Argentina).

References

- [1] G.S. Bales, A. Redfield, A. Zangwill, *Phys. Rev. Lett.* 62 (1989) 776.
- [2] M.A. Dubson, A. Jeffers, *Phys. Rev. B* 49 (1994) 8347.
- [3] J. Erlebacher, et al., *Phys. Rev. Lett.* 84 (2000) 5800.
- [4] W.W. Mullins, *J. Appl. Phys.* 30 (1959) 77.
- [5] See W. Selke, P.M. Duxbury, *Phys. Rev. B* 52 (1995) 17468 and references therein.
- [6] D.B. Abraham, *Comm. Math. Phys.* 49 (1976) 35.
- [7] D.B. Abraham, *Phys. Rev. Lett.* 47 (1981) 545.
- [8] W. Selke, T. Bieker, *Surf. Sci.* 281 (1993) 163.
- [9] W. Selke, P.M. Duxbury, *Z. Phys. B-Con. Mat.* 94 (1994) 311.
- [10] M.A. Dubson, G. Jeffers, *Phys. Rev. B* 49 (1994) 8347.
- [11] M.V. Ramana Murty, B.H. Cooper, *Scan. Microscopy* 12 (1998) 107.
- [12] G. Andreassen, P.L. Schilardi, O. Azzaroni, R.C. Salvarezza, *Langmuir* 18 (2002) 10430.
- [13] H.-C. Kan, S. Shah, T. Taddyon-Eslami, R.J. Phaneuf, *Phys. Rev. Lett.* 92 (2004) 146101.
- [14] H.P. Bonzel, E.E. Latta, *Surf. Sci.* 76 (1978) 225.
- [15] H.P. Bonzel, E. Preuss, *Surf. Sci.* 336 (1995) 225.
- [16] M. Giesen-Seibert, R. Jentjens, M. Poensgen, H. Ibach, *Phys. Rev. Lett.* 71 (1993) 3521.
- [17] M.F. Castez, R.C. Salvarezza, H.G. Solari, *Phys. Rev. E* 73 (2006) 011607.
- [18] M.F. Castez, E.V. Albano, *J. Phys. Chem. C* 111 (2007) 4606.
- [19] V. Tomar, M.R. Gungor, D. Maroudas, *Phys. Rev. Lett.* 100 (2008) 036106.
- [20] S. Katz, J.L. Lebowitz, H. Spohn, *Phys. Rev. B* 28 (1983) 1655.
- [21] N. Metropolis, A.W. Rosenbluth, M.M. Rosenbluth, A.H. Teller, E. Teller, *J. Chem. Phys.* 21 (1953) 1087.
- [22] B. Schmittmann, R.K.P. Zia, in: C. Domb, J. Lebowitz (Eds.), *Statistical Mechanics of Driven Diffusive System*, in: *Phase Transitions and Critical Phenomena*, vol. 17, Academic, London, 1995.
- [23] K.-t. Leung, *J. Stat. Phys.* 50 (1988) 405.
- [24] K.-t. Leung, K.K. Mon, J.L. Vallés, R.K.P. Zia, *Phys. Rev. Lett.* 61 (1988) 1744; *Phys. Rev. B* 39 (1989) 9312.
- [25] K.-t. Leung, R.K.P. Zia, *J. Phys. A: Math. Gen.* 26 (1993) L737.
- [26] R.K.P. Zia, K.-t. Leung, *J. Phys. A: Math. Gen.* 24 (1991) L1399.
- [27] G.P. Saracco, E.V. Albano, *Phys. Rev. E* 78 (2008) 031132.
- [28] A. Hernández-Machado, D. Jasnow, *Phys. Rev. A* 37 (1988) 656.
- [29] A. Hernández-Machado, H. Guo, J.L. Mozos, D. Jasnow, *Phys. Rev. A* 39 (1989) 4783.
- [30] D. Jasnow, R.K.P. Zia, *Phys. Rev. A* 36 (1987) 2243.
- [31] J.S. Langer, L.A. Turski, *Acta Metall.* 25 (1977) 1113.
- [32] D. Jasnow, D.A. Nicole, T. Ohta, *Phys. Rev. A* 23 (1981) 3192.
- [33] C. Yeung, J.L. Mozos, A. Hernández-Machado, D. Jasnow, *J. Stat. Phys.* 70 (1993) 1149.
- [34] G. Szabó, A. Solnoki, T. Antal, I. Borsos, *Fractals* 1 (1993) 954.
- [35] G. Szabó, *Phys. Rev. E* 49 (1994) 3508.
- [36] M. Kardar, G. Parisi, Y.-C. Zhang, *Phys. Rev. Lett.* 56 (1986) 889.
- [37] M. Díez-Minguito, P.L. Garrido, J. Marro, *Phys. Rev. E* 72 (2005) 026103.
- [38] P. Siders, *Phys. Rev. E* 79 (2009) 061101.
- [39] M.F. Castez, E.V. Albano, *J. Phys.: Condens. Mat.* 21 (2009) 263001.
- [40] E.V. Albano, V.C. Chappa, *Physica A* 327 (2003) 18; V.C. Chappa, E.V. Albano, *J. Chem. Phys.* 121 (2004) 328.
- [41] J.-F. Gouyet, M. Rosso, B. Sapoval, in: A. Bunde, S. Havlin (Eds.), *Fractals and Disordered Systems*, Springer-Verlag, Berlin, 1991; J. Kertsz, T. Vicsek, in: A. Bunde, S. Havlin (Eds.), *Fractals in Science*, Springer-Verlag, Berlin, 1995.
- [42] P.C. Hohenberg, B.I. Halperin, *Rev. Modern Phys.* 49 (1977) 435.
- [43] E.V. Albano, G. Saracco, *Phys. Rev. Lett.* 88 (2002) 145701.